JOURNAL OF GUIDANCE, CONTROL, AND DYNAMICS
Vol. 28, No. 5, September–October 2005

Singularity Escape/Avoidance Steering Logic for Control Moment Gyro Systems

Bong Wie*
Arizona State University, Tempe, Arizona 85287-6106

A singularity-robust control moment gyro (CMG) steering logic, developed previously, is a simple yet effective way of passing through, and also escaping from, any internal singularities. However, it is unable to escape the external saturation singularities of certain special CMG configurations, even when momentum desaturation is requested. Consequently, a new steering logic based on a mixed weighted two-norm and least-squares optimization solution is developed to overcome this deficiency of being trapped in the momentum saturation singularities. The new steering logic also provides a simple means of avoiding troublesome, internal elliptic singularities, which are commonly encountered by most pseudoinverse-based steering logic, including the previous singularity-robust steering logic. Although a CMG is a powerful torque amplification actuator, redundant CMG systems have an inherent geometric singularity problem, and consequently, transient torque errors are inevitable while escaping or passing through elliptic singularities. However, the resulting attitude transient dynamics are often acceptable because precision pointing is not required during large-angle slew maneuvers or CMG momentum desaturation maneuvers of most imaging satellites. Such slew maneuvers are usually performed by a closed-loop attitude control system, and thus, the steady-state pointing accuracy is not affected by such a CMG singularity problem.

I. Introduction

THE next-generation Earth imaging satellites will require rapid rotational agility as well as precision steady-state pointing accuracy for high-resolution images. Rather than sweep a gimbaled imaging system from side to side, the whole spacecraft body will turn rapidly. Pointing the entire spacecraft body allows the body-fixed imaging system to achieve a higher definition and improves the resolution for its images.

For example, the Pleiades high-resolution (HR) imaging satellite being developed by Centre National d'Etudes Spatiales/Astrium has a slew rate requirement of 4 deg/s. Because the overall cost and effectiveness of agile imaging satellites are greatly affected by the average retargeting time, the development of an agile attitude control system employing control moment gyros (CMGs) is of current practical importance.[1–5] As described in Refs. 1–3, the Pleiades-HR imaging satellite is equipped with four small single-gimbal CMGs of a pyramid arrangement with a skew angle of 30 deg. Each CMG has an angular momentum of 15 $\mathrm{N}\cdot\mathrm{m}\cdot\mathrm{s}$, a maximum gimbal rate of 3 rad/s, a peak output torque of 45 $\mathrm{N}\cdot\mathrm{m}$, and an average maximum torque of 20 $\mathrm{N}\cdot\mathrm{m}$. The 1000-kg Pleiades-HR imaging satellite with a roll/pitch inertia of approximately 800 $\mathrm{kg}\cdot\mathrm{m}^2$ will be able to perform a 60-deg roll (cross-track) slew maneuver in less than 25 s. It will provide a precision steady-state pointing accuracy of ± 0.03 deg during its planned imaging phase after completing the slew maneuver. However, during a large-angle cross-track slew maneuver, precision pointing of the spacecraft body is not required. The Pleiades-HR imaging satellite equipped with CMGs further justifies the development of a new CMG steering logic that can be simply integrated with a practical near-minimum-time slew control logic of Ref. 4. Such a CMG-based attitude/slew control system of agile imaging satellites is shown in Fig. 1.

For future scientific missions such as near-Earth object rendezvous and HR Earth observation using agile small satellites (<300 kg) with a slew rate requirement of 6 deg/s, a single-gimbal CMG (smaller than Astrium's CMG 15-45S) is currently under development at Surrey Space Centre.[5] Ball Aerospace is also currently developing an agile imaging satellite bus, BCP 5000, equipped with single-gimbal CMGs. The BCP 5000 is being developed to accommodate the next-generation optical and synthetic aperture radar remote-sensing payloads, and its CMG-based attitude control system will provide agile retargeting capability.

The use of CMGs necessitates the development of CMG steering logic that generates the CMG gimbal rate commands in response to the CMG torque commands, as shown in Fig. 1. One of the principal difficulties in using CMGs for spacecraft attitude control and momentum management is the geometric singularity problem in which no control torque is generated for the commanded control torques along a particular direction. At such a singularity, CMG torque is available in all but one direction. Such a classical singularity problem of CMGs has been reexamined recently in Ref. 6 to characterize and visualize the physical as well as mathematical nature of the singularities, singular momentum surfaces, and other singularity related problems. An extensive list of references dealing with the development of CMG singularity avoidance steering logic can be found in Ref. 6.

A simple yet effective way of passing through, and also escaping from, any internal singularities, as applied to agile spacecraft pointing control, has been developed recently in Refs. 7 and 8. The CMG steering logic of Refs. 7 and 8 is mainly intended for typical large-angle slew maneuvers in which precision pointing or tracking is not required during slew maneuvers, and it fully uses the available CMG momentum space in the presence of any singularities. Because the singularity-robust steering logic developed in Refs. 7 and 8 is based on the minimum two-norm, pseudoinverse solution, it does not explicitly avoid singularity encounters, but it rather approaches and rapidly transits unavoidable singularities whenever needed. It effectively generates deterministic dither signals when the system is nearly singular. Any internal singularities can be escaped for any nonzero constant torque commands using the singularity-robust steering logic.

However, this paper will show that the CMG steering logic of Refs. 7 and 8 is unable to escape the saturation singularities of certain CMG configurations, which can be problematic if CMG momentum desaturation is desired. Consequently, a new steering logic is developed to overcome this deficiency of the singularity-robust CMG steering logic of Refs. 7 and 8. The new steering logic uses an additional weighting matrix in conjunction with the

Presented as Paper 2003-5659 at the Guidance, Navigation, and Control Conference, Austin, TX, 11–14 August 2003; received 14 April 2004; revision received 27 April 2004; accepted for publication 27 April 2004.

*Professor, Department of Mechanical and Aerospace Engineering; bong.wie@asu.edu. Associate Fellow AIAA.

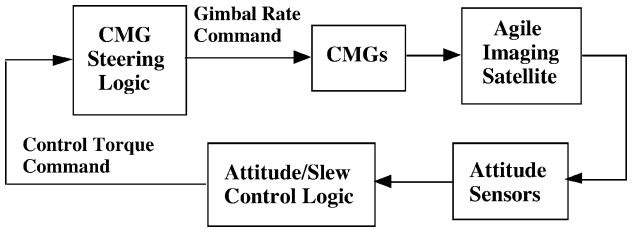

Fig. 1 CMG-based attitude/slew control system of agile imaging satellites.

deterministic dither signals employed in Refs. 7 and 8. It can also be employed to avoid singularity encounters explicitly for which most other pseudoinverse-based steering logic either fail or must transit through. The new steering logic is simple to implement, compared to other explicit singularity-avoidance algorithms employing gradient methods, global search, optimization, and/or null motion. It is again emphasized that the previous singularity-robust steering logic,[7,8] as well as the new steering logic, is mainly intended for most practical situations in which precision pointing or tracking is not required during large-angle slew maneuvers, CMG momentum desaturation, and CMG reconfiguration.

The remainder of this paper is briefly outlined as follows. In Sec. II, a brief summary is provided of the standard pseudoinverse-based steering logic that the proposed new steering logic is based on. In Sec. III, the new singularity escape/avoidance steering logic that significantly enhances the previous singularity-robust steering logic of Refs. 7 and 8 is described. In Sec. IV, the simplicity and effectiveness of the new steering logic will be demonstrated using various CMG systems, such as two or three parallel single-gimbal CMG configurations, a pyramid array of four single-gimbal CMGs of the Pleiades-HR imaging satellite, and four parallel double-gimbal CMGs of the International Space Station.

II. Standard Pseudoinverse Steering Logic

Consider a CMG torque model simply given by

$$\boldsymbol{A}\dot{\boldsymbol{x}} = \boldsymbol{\tau} \tag{1}$$

where $\boldsymbol{A}$ is a $3 \times n$ Jacobian matrix, $\dot{\boldsymbol{x}} = (\dot{x}_1, \ldots, \dot{x}_n)$, and x_i is the ith gimbal angle. For the given control torque command $\boldsymbol{\tau}$, a gimbal rate command $\dot{\boldsymbol{x}}$, often referred to as the pseudoinverse steering logic, is then obtained as

$$\dot{\boldsymbol{x}} = \boldsymbol{A}^{+}\boldsymbol{\tau} \tag{2}$$

where

$$\boldsymbol{A}^{+} = \boldsymbol{A}^{T}(\boldsymbol{A}\boldsymbol{A}^{T})^{-1} \tag{3}$$

This pseudoinverse is the minimum two-norm solution of the following constrained minimization problem:

$$\min_{\dot{x}} \|\dot{\boldsymbol{x}}\|^2 \qquad \text{subject to} \qquad \boldsymbol{A}\dot{\boldsymbol{x}} = \boldsymbol{\tau} \tag{4}$$

where $\|\dot{\boldsymbol{x}}\|^2 = \dot{\boldsymbol{x}}^T\dot{\boldsymbol{x}}$. Most CMG steering laws determine the gimbal rate commands with some variant of the pseudoinverse of the form (3).

The pseudoinverse is a special case of the weighted minimum two-norm solution

$$\dot{\boldsymbol{x}} = \boldsymbol{A}^{+}\boldsymbol{\tau} \qquad \text{where} \qquad \boldsymbol{A}^{+} = \boldsymbol{Q}^{-1}\boldsymbol{A}^{T}[\boldsymbol{A}\boldsymbol{Q}^{-1}\boldsymbol{A}^{T}]^{-1} \tag{5}$$

of the following constrained minimization problem:

$$\min_{\dot{x}} \|\dot{\boldsymbol{x}}\|_Q^2 \qquad \text{subject to} \qquad \boldsymbol{A}\dot{\boldsymbol{x}} = \boldsymbol{\tau} \tag{6}$$

where $\|\dot{\boldsymbol{x}}\|_Q^2 = \dot{\boldsymbol{x}}^T\boldsymbol{Q}\dot{\boldsymbol{x}}$ and $\boldsymbol{Q} = \boldsymbol{Q}^T > 0$. Later in this paper, the significance of choosing $\boldsymbol{Q} \neq \boldsymbol{I}$, where $\boldsymbol{I}$ is an identity matrix, will be demonstrated. However, $\boldsymbol{Q} \neq \boldsymbol{I}$ alone does not resolve the singularity problem also inherent in Eq. (5).

If rank $(\boldsymbol{A}) < m$ for certain sets of gimbal angles, or equivalently rank $(\boldsymbol{A}\boldsymbol{A}^T) < m$, when $\boldsymbol{A}$ is an $m \times n$ matrix, the pseudoinverse does not exist, and it is said that the pseudoinverse steering logic encounters singular states. This singular situation occurs when all individual CMG torque output vectors are perpendicular to the commanded torque direction. Equivalently, the singular situation occurs when all individual CMG momentum vectors have extremal projections onto the commanded torque $\boldsymbol{\tau}$.

Because the pseudoinverse $\boldsymbol{A}^{+} = \boldsymbol{A}^{T}(\boldsymbol{A}\boldsymbol{A}^{T})^{-1}$ is the minimum two-norm solution of gimbal rates subject to the constraint $\boldsymbol{A}\dot{\boldsymbol{x}} = \boldsymbol{\tau}$, the pseudoinverse steering logic and all other pseudoinverse-based steering logic tend to leave inefficiently positioned CMGs alone causing the gimbal angles to eventually "hang-up" in antiparallel singular arrangements. That is, they tend to steer the gimbals toward antiparallel singular states. Despite this deficiency, the pseudoinverse steering logic, or some variant of pseudoinverse, is commonly employed for most CMG systems because of its simplicity for onboard, real-time implementation.[9]

III. Singularity Escape/Avoidance Steering Logic

The singularity-robust CMG steering logic[7,8] was mainly intended for most practical situations in which precision pointing or tracking is not required during large-angle slew maneuvers, and it fully utilizes the available CMG momentum space in the presence of any singularities. It has the following form:

$$\dot{\boldsymbol{x}} = \boldsymbol{A}^{\#}\boldsymbol{\tau} \tag{7}$$

where

$$\boldsymbol{A}^{\#} = [\boldsymbol{A}^T\boldsymbol{P}\boldsymbol{A} + \lambda\boldsymbol{I}]^{-1}\boldsymbol{A}^T\boldsymbol{P} = \boldsymbol{A}^T[\boldsymbol{A}\boldsymbol{A}^T + \lambda\boldsymbol{E}]^{-1} \tag{8}$$

$$\boldsymbol{P}^{-1} \equiv \boldsymbol{E} = \begin{bmatrix} 1 & \epsilon_3 & \epsilon_2 \\ \epsilon_3 & 1 & \epsilon_1 \\ \epsilon_2 & \epsilon_1 & 1 \end{bmatrix} > 0 \tag{9}$$

The positive scalar λ and the off-diagonal elements ϵ_i are to be properly selected such that $\boldsymbol{A}^{\#}\boldsymbol{\tau} \neq 0$ for any nonzero constant $\boldsymbol{\tau}$.

Note that there exists always a null vector of $\boldsymbol{A}^{\#}$ because rank$(\boldsymbol{A}^{\#}) < 3$ for any λ and ϵ_i when the Jacobian matrix $\boldsymbol{A}$ is singular. Consequently, a simple way of guaranteeing that $\boldsymbol{A}^{\#}\boldsymbol{\tau} \neq 0$ for any nonzero constant $\boldsymbol{\tau}$ command is to modulate ϵ_i continuously, for example, as follows:

$$\epsilon_i = \epsilon_0 \sin(\omega t + \phi_i) \tag{10}$$

where the amplitude ϵ_0, the modulation frequency ω, and the phases ϕ_i need to be appropriately selected. The scalar λ may be adjusted as

$$\lambda = \lambda_o \exp[-\mu \det(\boldsymbol{A}\boldsymbol{A}^T)] \tag{11}$$

where λ_o and μ are constants to be properly selected.

Any internal singularities can be escaped for any nonzero constant torque commands using the singularity-robust steering logic. However, some external saturation singularities of certain special CMG configurations cannot be escaped for any choice of λ and ϵ_i, as will be shown later. Consequently, a new steering logic, which is capable of escaping all types of singularities, is proposed as follows[10]:

$$\dot{\boldsymbol{x}} = \boldsymbol{A}^{\#}\boldsymbol{\tau} \tag{12}$$

where

$$\begin{aligned} \boldsymbol{A}^{\#} &= [\boldsymbol{A}^T\boldsymbol{P}\boldsymbol{A} + \boldsymbol{Q}]^{-1}\boldsymbol{A}^T\boldsymbol{P} \\ &\equiv \boldsymbol{Q}^{-1}\boldsymbol{A}^T[\boldsymbol{A}\boldsymbol{Q}^{-1}\boldsymbol{A}^T + \boldsymbol{P}^{-1}]^{-1} \\ &\equiv \boldsymbol{W}\boldsymbol{A}^T[\boldsymbol{A}\boldsymbol{W}\boldsymbol{A}^T + \boldsymbol{V}]^{-1} \end{aligned} \tag{13}$$

where $\boldsymbol{W} \equiv \boldsymbol{Q}^{-1}$ and $\boldsymbol{V} \equiv \boldsymbol{P}^{-1}$. For a $3 \times n$ Jacobian matrix $\boldsymbol{A}$, $[\boldsymbol{A}^T\boldsymbol{P}\boldsymbol{A} + \boldsymbol{Q}]$ is an $n \times n$ matrix and $[\boldsymbol{A}\boldsymbol{W}\boldsymbol{A}^T + \boldsymbol{V}]$ is a 3×3 matrix.

The singularity-robust inverse of the form (13) is the solution of the well-known, mixed two-norm and least-squares minimization problem:

$$\min_{\dot{x}}(\boldsymbol{e}^T\boldsymbol{P}\boldsymbol{e}+\dot{\boldsymbol{x}}^T\boldsymbol{Q}\dot{\boldsymbol{x}}) \tag{14}$$

where $\boldsymbol{e}=\boldsymbol{A}\dot{\boldsymbol{x}}-\boldsymbol{\tau}$ is the torque error vector. Because $\boldsymbol{P}$ and $\boldsymbol{Q}$ are positive definite matrices, $[\boldsymbol{A}^T\boldsymbol{P}\boldsymbol{A}+\boldsymbol{Q}]$ and $[\boldsymbol{A}\boldsymbol{W}\boldsymbol{A}^T+\boldsymbol{V}]$ are always nonsingular.

The weighting matrices $\boldsymbol{P}$ and $\boldsymbol{Q}$ (equivalently, $\boldsymbol{W}$ and $\boldsymbol{V}$) must be properly chosen 1) to obtain acceptable levels of torque errors and gimbal rates, 2) to escape any internal as well as external singularities, and 3) to pass through singularities or avoid singularity encounters.

For example, $\boldsymbol{P}$ is chosen such that $\boldsymbol{A}^T\boldsymbol{P}\boldsymbol{\tau}\neq 0$ for any torque command $\boldsymbol{\tau}$, as follows:

$$\boldsymbol{P}^{-1}\equiv\boldsymbol{V}=\lambda\begin{bmatrix}1 & \epsilon_3 & \epsilon_2\\ \epsilon_3 & 1 & \epsilon_1\\ \epsilon_2 & \epsilon_1 & 1\end{bmatrix}>0 \tag{15}$$

and λ and ϵ_i are appropriately selected as discussed earlier.

Because the condition $\boldsymbol{A}^T\boldsymbol{P}\boldsymbol{\tau}\neq 0$, which is a necessary condition, is not sufficient for escaping and/or avoiding singularities, the matrix $\boldsymbol{Q}$ also needs to be properly chosen as

$$\boldsymbol{Q}^{-1}\equiv\boldsymbol{W}=\begin{bmatrix}W_1 & \lambda & \lambda & \lambda\\ \lambda & W_2 & \lambda & \lambda\\ \lambda & \lambda & W_3 & \lambda\\ \lambda & \lambda & \lambda & W_4\end{bmatrix}>0 \tag{16}$$

for a case of $n=4$. Different values of W_i and/or nonzero off-diagonal elements are required to escape all types of singularities, including the external saturation singularities when CMG momentum desaturation is requested. Furthermore, a proper choice of $\boldsymbol{W}\neq\boldsymbol{I}$ provides an effective means for explicitly avoiding singularity encounters (to be demonstrated in the next section).

Several examples of demonstrating the significance of $\boldsymbol{W}\neq\boldsymbol{I}$ for escaping a certain type of external saturation singularities for which the previous singularity-robust steering logic of Refs. 7 and 8 fails will be presented in the next section. Examples of avoiding an internal elliptic singularity, which the previous singularity-robust steering logic had to pass through, will also be presented in the next section.

IV. Illustrative Examples

In this section, the simplicity and effectiveness of the new steering logic will be demonstrated using various CMG systems, such as two or three parallel single-gimbal CMG configuration, a pyramid array of four single-gimbal CMGs, and four parallel double-gimbal CMGs of the International Space Station. Notice in various simulation results of this section that transient CMG torque errors are inevitable while escaping or passing through elliptic singularities. However, the resulting attitude transient dynamics are often acceptable because precision pointing is not required during large-angle slew maneuvers or CMG momentum desaturation maneuvers of most imaging satellites. Such slew maneuvers are usually performed by a closed-loop attitude control system as shown in Fig. 1, and thus, the steady-state pointing accuracy is not affected by such a CMG singularity problem.

Two Parallel Single-Gimbal CMGs

Most agile imaging satellites, such as the Earth-observing satellite require large control torques only along the roll and pitch axes, not along the Earth-pointing yaw axis. For such a case, two or three single-gimbal CMGs with parallel gimbal axes can be employed for the roll/pitch control of an Earth-observing spacecraft, whereas the yaw axis is controlled by a smaller reaction wheel.

For a system of two CMGs without redundancy, the momentum vectors, $\boldsymbol{h}_1$ and $\boldsymbol{h}_2$ move in the (x, y) plane normal to the gimbal axis,

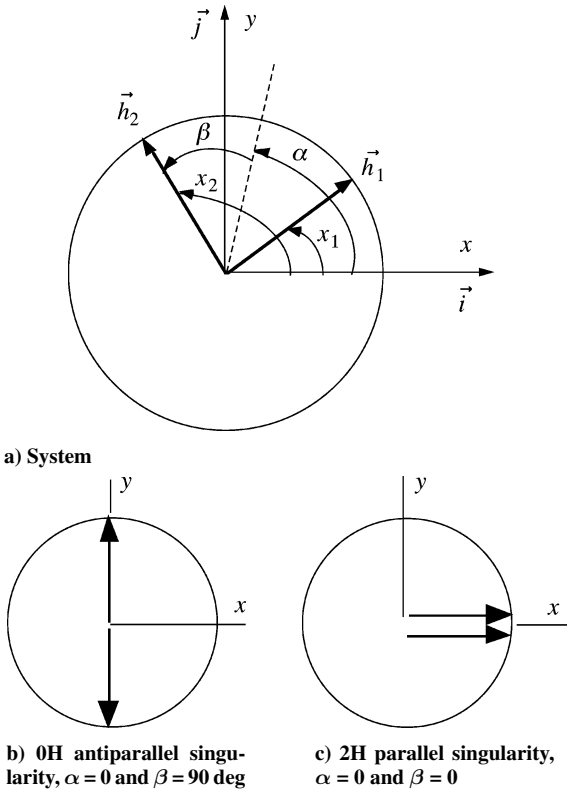

Fig. 2 Two SGCMGs with parallel gimbal axes, which remains singular for any α motion when β = 0 or 90 deg.

as shown in Fig. 2a. For such "scissored" single-gimbal CMGs, the total CMG momentum vector is simply represented as

$$\boldsymbol{H}=\begin{bmatrix}\cos x_1+\cos x_2\\ \sin x_1+\sin x_2\end{bmatrix} \tag{17}$$

where a constant unit momentum for each CMG is assumed.

Define a new set of gimbal angles α and β as follows:

$$\alpha=(x_1+x_2)/2, \qquad \beta=(x_2-x_1)/2 \tag{18}$$

where α is called the rotation angle and β the scissor angle. We obtain

$$\boldsymbol{H}=2\begin{bmatrix}\cos\alpha\cos\beta\\ \sin\alpha\cos\beta\end{bmatrix} \tag{19}$$

$$\dot{\boldsymbol{H}}=\boldsymbol{A}\dot{\boldsymbol{x}} \tag{20}$$

where $\dot{\boldsymbol{H}}=(\dot{H}_x, \dot{H}_y)$, $\dot{\boldsymbol{x}}=(\dot{\alpha}, \dot{\beta})$, and $\boldsymbol{A}$ is the Jacobian matrix defined as

$$\boldsymbol{A}=2\begin{bmatrix}-\sin\alpha\cos\beta & -\cos\alpha\sin\beta\\ \cos\alpha\cos\beta & -\sin\alpha\sin\beta\end{bmatrix} \tag{21}$$

For the internal antiparallel singularity at $\boldsymbol{x}=(\alpha, \beta)=(0, \pi/2)$, shown in Fig. 2b, the Jacobian matrix becomes

$$\boldsymbol{A}=\begin{bmatrix}0 & -2\\ 0 & 0\end{bmatrix}$$

with its singular vector $\boldsymbol{u}=(0, 1)$, that is $\boldsymbol{A}^T\boldsymbol{u}=0$. A null space vector of $\boldsymbol{A}$ such that $\boldsymbol{A}\dot{\boldsymbol{x}}=0$ is $\dot{\boldsymbol{x}}=\text{null}\,(\boldsymbol{A})=(1, 0)$.

Although null motion does exist from this singularity, this hyperbolic singularity cannot be escaped by null motion because the singular configuration $(\beta=\pi/2)$ remains undisturbed during this null motion along the null manifold (or a degenerate trajectory). Although null motion can be generated at this hyperbolic singularity,

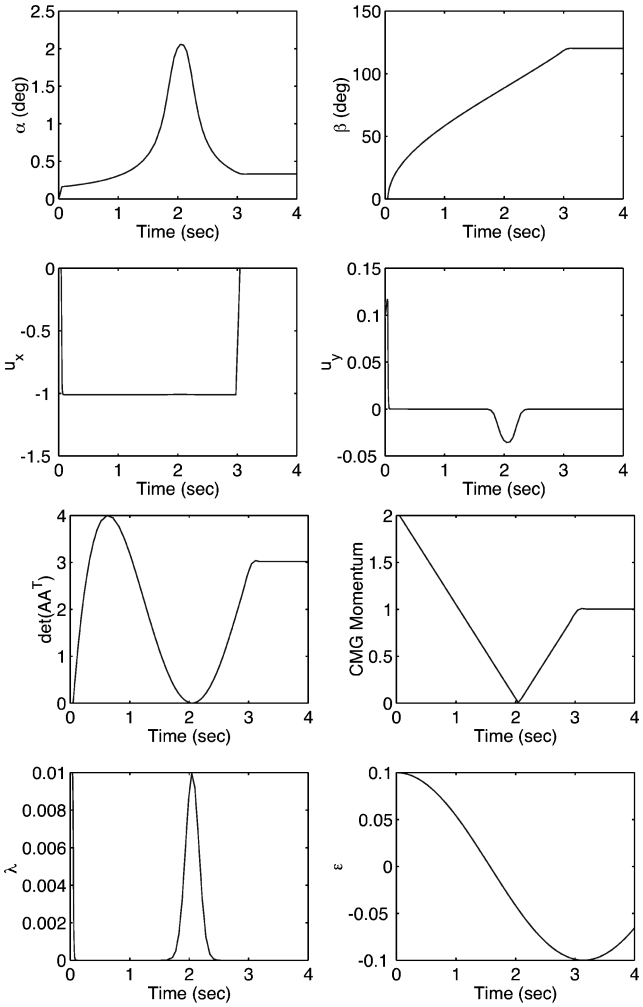

Fig. 3 Singularity escape (momentum desaturation) simulation results for two parallel SGCMGs with proposed new steering logic.

this example demonstrates that the mere existence of null motion does not guarantee escape from a singularity. However, this type of internal singularity can be easily escaped by the singularity-robust steering logic of Refs. 7 and 8.

For the saturation singularity at $\boldsymbol{x} = (\alpha, \beta) = (0, 0)$, shown in Fig. 2c, the Jacobian matrix becomes

$$\boldsymbol{A} = \begin{bmatrix} 0 & 0 \\ 2 & 0 \end{bmatrix}$$

with its singular vector $\boldsymbol{u} = (-1, 0)$ and its null space vector $\dot{\boldsymbol{x}} = \text{null}(\boldsymbol{A}) = (0, 1)$. This external elliptic singularity cannot be escaped by null motion because null motion does not exist in the vicinity of this momentum saturation singularity.

The singularity-robust inverse with λ and $\epsilon = 0.1$ becomes

$$\boldsymbol{A}^{\#} = \boldsymbol{A}^T[\boldsymbol{A}\boldsymbol{A}^T + 0.1\boldsymbol{E}]^{-1} = \begin{bmatrix} -0.0488 & 0.4879 \\ 0 & 0 \end{bmatrix}$$

$$\Rightarrow \dot{\boldsymbol{x}} = \boldsymbol{A}^{\#}\begin{bmatrix} -1 \\ 0 \end{bmatrix} = \begin{bmatrix} 0.0488 \\ 0 \end{bmatrix}$$

Note that $\dot{\boldsymbol{x}} = (\dot{\alpha}, \dot{\beta}) \neq 0$, but $\dot{\beta} = 0$, that is, the system remains singular while α changes. In fact, $\dot{\beta} = 0$ for any torque command vector $\boldsymbol{\tau}$ and any ϵ_i. Consequently, the singularity-robust steering logic of Refs. 7 and 8 is unable to command a nonzero $\dot{\beta}$ for this special case.

However, this external singularity can be escaped by the new singularity escape/avoidance steering logic, proposed in this paper, of the form $\dot{\boldsymbol{x}} = \boldsymbol{A}^{\#}\boldsymbol{\tau}$ where

$$\boldsymbol{A}^{\#} = \boldsymbol{W}\boldsymbol{A}^T[\boldsymbol{A}\boldsymbol{W}\boldsymbol{A}^T + \boldsymbol{V}]^{-1}$$

As can be seen in Fig. 3, the momentum saturation singularity is escaped using the new steering logic with

$$\boldsymbol{V} = \lambda\begin{bmatrix} 1 & \epsilon \\ \epsilon & 1 \end{bmatrix}, \qquad \boldsymbol{W} = \begin{bmatrix} 1 & \lambda \\ \lambda & 1 \end{bmatrix}$$

where $\epsilon = 0.1\cos t$ and $\lambda = 0.01\exp[-10\det(\boldsymbol{A}\boldsymbol{A}^T)]$.

In Fig. 3, (u_x, u_y) are the actual torques generated by the CMG system for the commanded torques of $(\tau_x, \tau_y) = (-1, 0)$ for $0 \le t \le 3$ s. The CMG momentum is completely desaturated at $t = 2$ s, but the desaturation torque is commanded until $t = 3$ s to explore further any problem of encountering an internal singularity. (For all of the simulation results presented in this paper, the commanded torque level, as well as the CMG momentum, is normalized as one without loss of generality. Thus, it should be appropriately adjusted depending on the actual values of gimbal rate limit and CMG momentum magnitude.) As can be seen in Fig. 3, the new steering logic also provides a simple yet effective way of passing through the 0H internal hyperbolic singularity, but with a small transient torque error in u_y, which is inevitable while passing through the hyperbolic singularity.

Note that for this special case of two parallel single-gimbal CMGs, there exists a direct inverse solution. A steering logic based on the direct inverse of $\boldsymbol{A}$ can be obtained for this simple 2×2 problem as follows:

$$\dot{\boldsymbol{x}} = \boldsymbol{A}^{-1}\boldsymbol{\tau} \tag{22}$$

where

$$\boldsymbol{A}^{-1} = \frac{1}{2|\boldsymbol{A}|}\begin{bmatrix} -\sin\alpha\cos\beta & -\cos\alpha\sin\beta \\ \cos\alpha\cos\beta & -\sin\alpha\sin\beta \end{bmatrix} = \frac{1}{2}\begin{bmatrix} -\sin\alpha/\cos\beta & \cos\alpha/\cos\beta \\ -\cos\alpha/\sin\beta & -\sin\alpha/\sin\beta \end{bmatrix} \tag{23}$$

Then, we obtain

$$\dot{\alpha} = \frac{-\sin\alpha\tau_x + \cos\alpha\tau_y}{2(\cos\beta + \lambda_1)} \tag{24}$$

$$\dot{\beta} = \frac{-\cos\alpha\tau_x - \sin\alpha\tau_y}{2(\sin\beta + \lambda_2)} \tag{25}$$

where

$$\lambda_1 = \lambda_o\exp[-\mu\det(\boldsymbol{A}\boldsymbol{A}^T)]\sin\beta \tag{26a}$$

$$\lambda_2 = \lambda_o\exp[-\mu\det(\boldsymbol{A}\boldsymbol{A}^T)]\cos\beta \tag{26b}$$

which are included in the steering law to avoid dividing by zero when the system becomes singular.

As shown in Fig. 4, the momentum saturation singularity is easily escaped using this direct-inverse steering logic for $(\tau_x, \tau_y) = (-1, 0)$ for $0 \le t \le 3$ s with $\lambda_0 = 0.01$ and $\mu = 10$. In Fig. 4, (u_x, u_y) are the actual torques generated by the CMG system for the commanded torques: $(\tau_x, \tau_y) = (-1, 0)$ for $0 \le t \le 3$ s. It can be seen that this direct inverse steering logic provides a very smooth transit through the 0H internal singularity, without any torque transient error.

However, such an exact direct-inverse steering logic does not exist for the practical cases with redundant CMGs, as discussed in the remainder of this section.

Three Parallel Single-Gimbal CMGs

For a system of three single-gimbal CMGs with parallel gimbal axes, $\boldsymbol{W}$ should be selected as $W_1 \neq W_2 \neq W_3$ to escape the 3H saturation singularity at $(x_1, x_2, x_3) = (0, 0, 0)$ with $(\tau_x, \tau_y) = (-1, 0)$, whereas $\boldsymbol{V} = \lambda\boldsymbol{E}$ is simply selected as $\epsilon_i = 0.1\cos t$ and $\lambda = 0.01\exp[-10\det(\boldsymbol{A}\boldsymbol{A}^T)]$. Simulation results

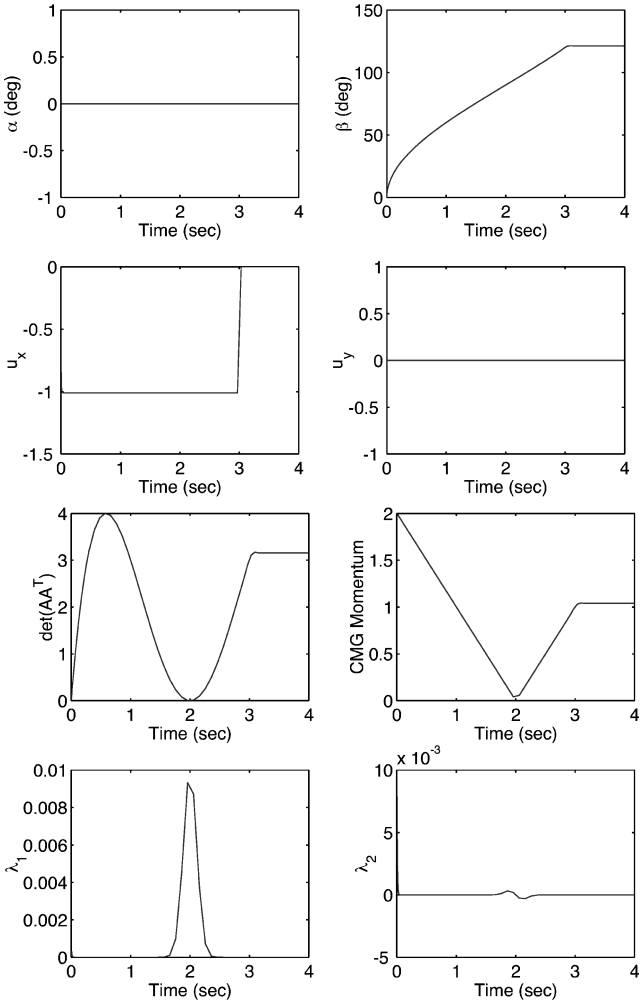

Fig. 4 Singularity escape (momentum desaturation) simulation results for two parallel SGCMGs with direct-inverse steering logic.

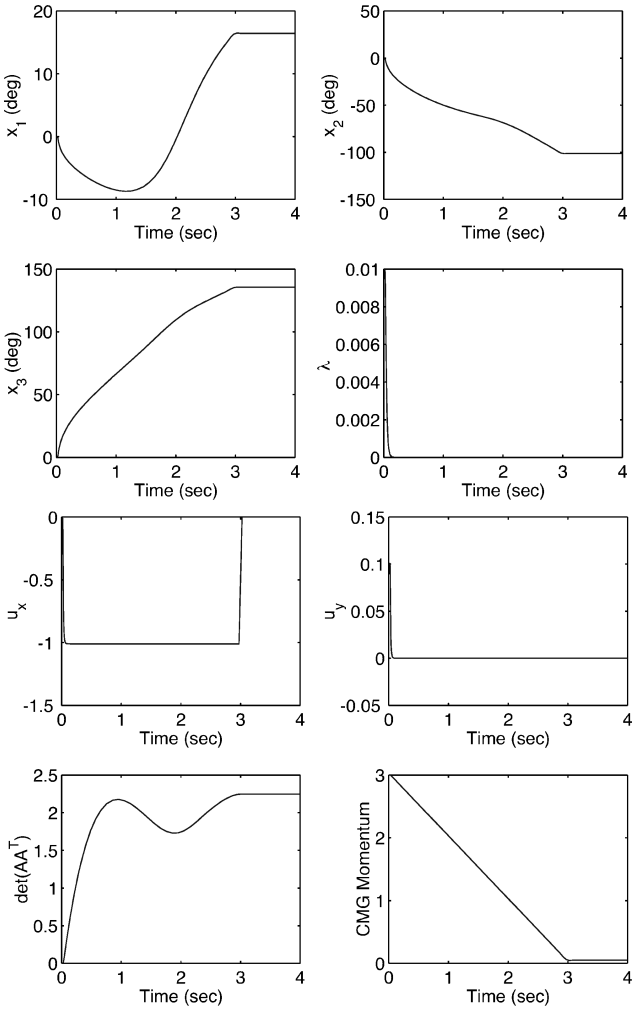

Fig. 5 Singularity escape (momentum desaturation) simulation results for three parallel SGCMGs with the proposed steering logic of $W = \mathbf{diag}\{1, 2, 3\}$.

of $(\tau_x, \tau_y) = (-1, 0)$ for $0 \le t \le 3$ s with $\boldsymbol{W} = \mathrm{diag}\{1, 2, 3\}$ are shown in Fig. 5. Detailed discussion of this system of three single-gimbal CMGs with parallel gimbal axes may be found in Ref. 6.

Pyramid Array of Four Single-Gimbal CMGs

For a typical pyramid mount of four single-gimbal CMGs with skew angle of β, shown in Fig. 6, we have the Jacobian matrix as

$$\boldsymbol{A} = \begin{bmatrix} -c\beta\cos x_1 & \sin x_2 & c\beta\cos x_3 & -\sin x_4 \\ -\sin x_1 & -c\beta\cos x_2 & \sin x_3 & c\beta\cos x_4 \\ s\beta\cos x_1 & s\beta\cos x_2 & s\beta\cos x_3 & s\beta\cos x_4 \end{bmatrix} \tag{27}$$

where x_i is the ith gimbal angle, $c\beta \equiv \cos\beta$, and $s\beta \equiv \sin\beta$.

The Pleiades-HR imaging satellite[1–3] will be controlled by a pyramid cluster of four small single-gimbal CMGs. The z axis of the pyramid cluster, shown in Fig. 6, is aligned along the line of sight of the Earth-pointing optical imaging system of Pleiades-HR imaging satellite, and a 30-deg skew angle is selected to have a larger angular momentum capability along the x and y axes.

When $\beta = 90$ deg, we have a four-CMG configuration with two orthogonal pairs of scissored CMGs. This case is also of practical importance due to its simple arrangement of four single-gimbal CMGs for three-axis control applications. Similar to the case of three parallel single-gimbal CMGs, $\boldsymbol{W} \neq \boldsymbol{I}$ is also required to escape the saturation singularity (Fig. 7). For this simulation, $\boldsymbol{W} = \mathrm{diag}\{1, 2, 3, 4\}$ and $\boldsymbol{V} = \lambda\boldsymbol{E}$ with $\epsilon_i = 0.1\cos t$ and $\lambda = 0.01\exp[-10\det(\boldsymbol{A}\boldsymbol{A}^T)]$ were used to escape the saturation singularity at $(\pi/2, \pi/2, \pi/2, \pi/2)$ with $(\tau_x, \tau_y, \tau_z) = (0, 0, -1)$ for

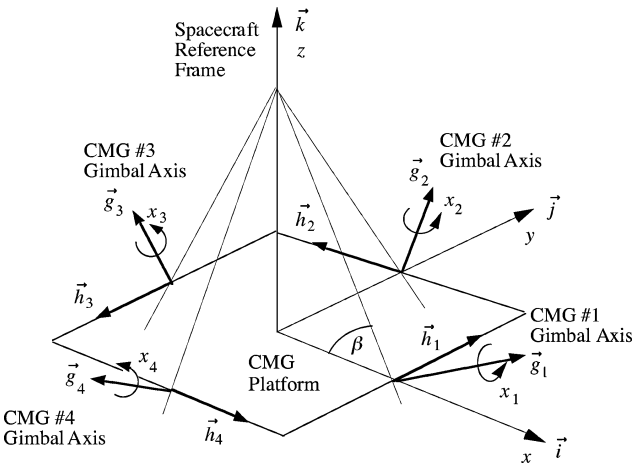

Fig. 6 Pyramid mounting arrangement of four SGCMGs.

$0 \le t \le 4$ s. It can be seen in Fig. 7 that an internal singularity is encountered at $t = 2$ s, but it is rapidly passed through.

For all other simulation results presented in the remainder of this paper, $\boldsymbol{V} = \lambda\boldsymbol{E}$ with $\epsilon_i = 0.1\cos t$ and $\lambda = 0.01\exp[-10\det(\boldsymbol{A}\boldsymbol{A}^T)]$ were used.

In Fig. 8, simulation results are shown for a typical pyramid array of four single-gimbal CMGs ($\beta = 53.13$ deg) with initial gimbal angles of (0, 0, 0, 0) and a torque command of $(\tau_x, \tau_y, \tau_z) = (1, 0, 0)$.

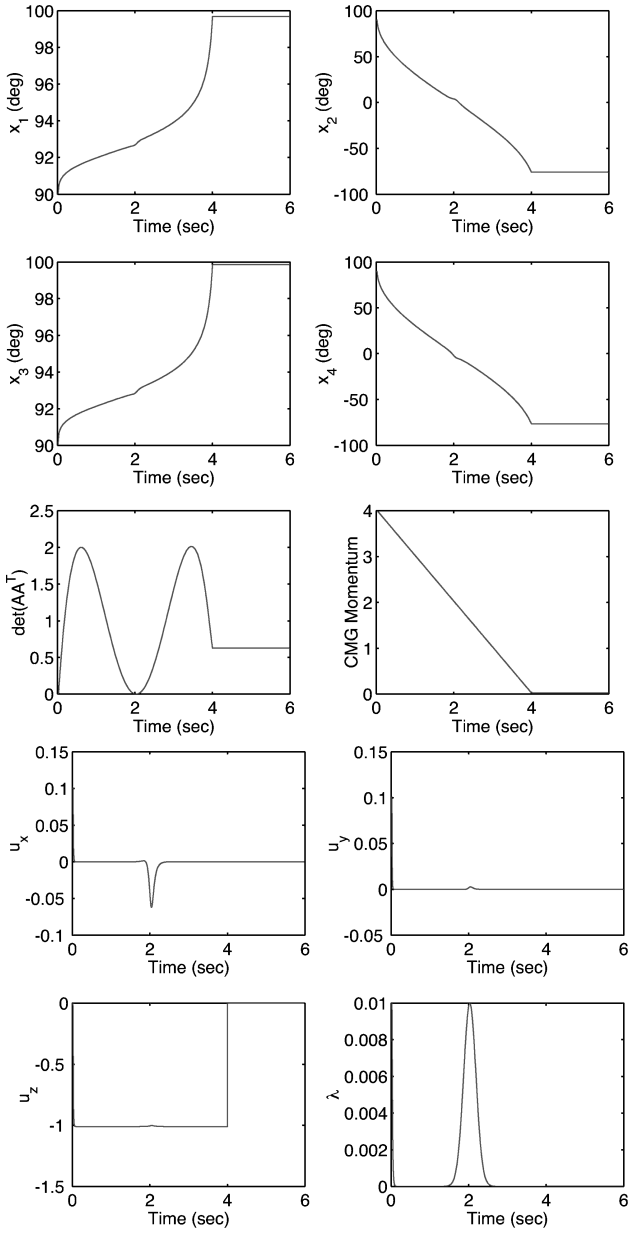

Fig. 7 Singularity escape (momentum desaturation) simulation for four SGCMGs (β = π/2) with proposed steering logic of W = diag {1, 2, 3, 4}.

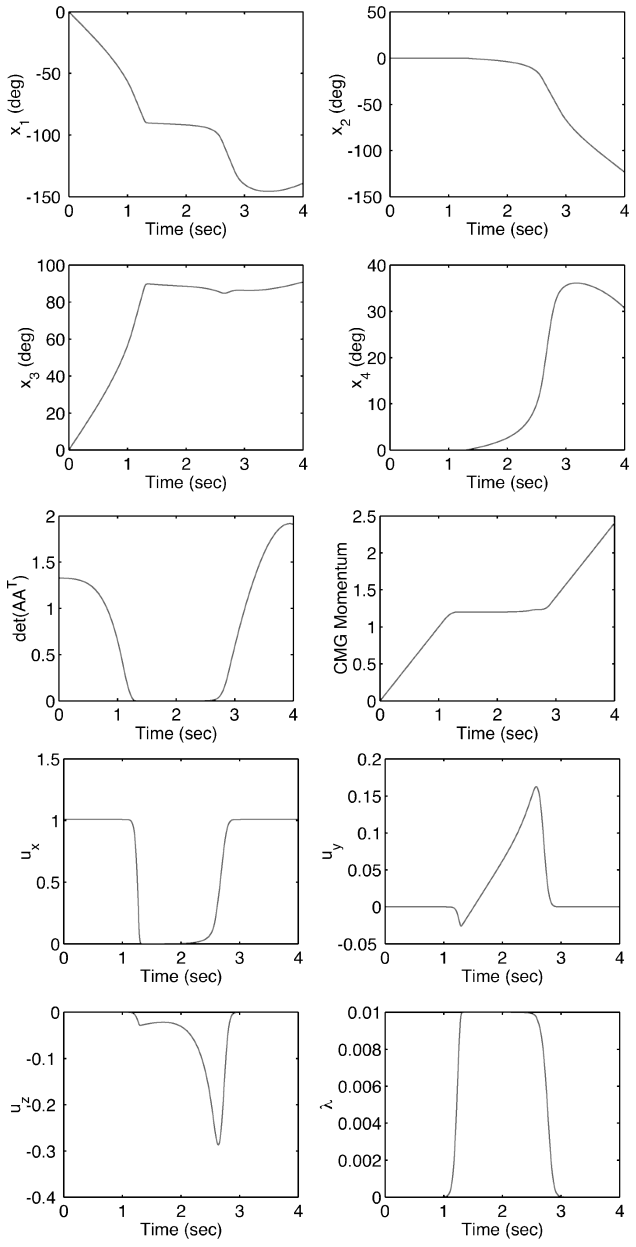

Fig. 8 Typical roll torque command test case for four SGCMGs (β = 53.13 deg), starting from nonsingular, zero-initial gimbal angles and passing through well-known internal elliptic singularity, with the previous steering logic of Refs. 7 and 8 with W = diag{1, 1, 1, 1}.

For this typical roll torque command simulation with zero initial gimbal angles, $\boldsymbol{W} = \text{diag}\{1, 1, 1, 1\}$ was used, that is, the singularity-robust steering logic of Refs. 7 and 8 was used for this simulation. It can be seen that the well-known internal elliptic singularity at $(-\pi/2, 0, \pi/2, 0)$ is encountered, but it is successfully passed through. The inevitable transient torque errors during the singularity transit can be seen in Fig. 8.

In Fig. 9, simulation results with $\boldsymbol{W} = \text{diag}\{10^{-4}, 1, 1, 1\}$ are shown for the earlier case of a typical pyramid array of four single-gimbal CMGs ($\beta = 53.13$ deg) with initial gimbal angles of $(0, 0, 0, 0)$ and a torque command of $(\tau_x, \tau_y, \tau_z) = (1, 0, 0)$. It can be seen that the well-known internal elliptic singularity at $(-\pi/2, 0, \pi/2, 0)$ is not directly encountered. However, the inevitable transient torque errors, caused by skirting such a troublesome, impassable elliptic singularity, can also be seen in Fig. 9. A different weighting matrix of $\boldsymbol{W} = \text{diag}\{1, 1, 10^{-4}, 1\}$ can also be employed for this case.

For the simulations shown in Figs. 8 and 9, the maximum gimbal rate of each CMG was explicitly limited to ± 2 rad/s. Such a gimbal rate saturation limit did not affect the singularity-avoidance performance of the proposed steering logic. The gimbal-rate time histories associated with the simulation shown in Fig. 9 are provided in Fig. 10. Although the gimbal rate command is limited to ± 2 rad/s, the gimbal angle and CMG torque time histories shown in Fig. 9 are all acceptable.

Four Parallel Double-Gimbal CMGs

The simplicity and effectiveness of the proposed steering logic will be demonstrated here also for a system of double-gimbal CMGs (DGCMG). For a DGCMG, the rotor is suspended inside two gimbals, and consequently, the rotor momentum can be oriented on a sphere along any direction provided no restrictive gimbal stops. For the different purposes of redundancy management and failure accommodation, several different arrangements of DGCMGs have been developed, such as three orthogonally mounted DGCMGs used in the Skylab and four parallel mounted DGCMGs employed for the International Space Station.

As shown by Kennel,[11] mounting of DGCMGs of unlimited outer gimbal angle freedom with all their outer gimbal axes parallel allows drastic simplification of the CMG steering law development

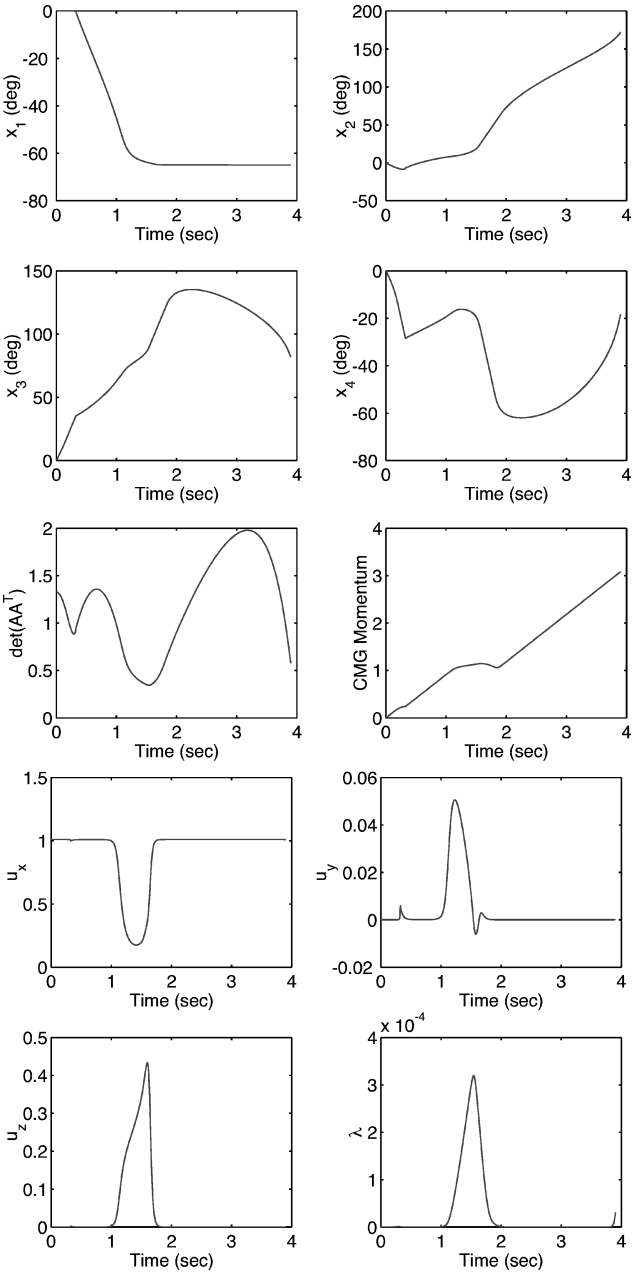

Fig. 9 Typical roll torque command test case for four SGCMGs (β = 53.13 deg), starting from nonsingular, zero-initial gimbal angles and new steering logic of W = diag$\{10^{-4}, 1, 1, 1\}$.

in the redundancy management and failure accommodation and in the mounting hardware.

Consider such a parallel mounting arrangement of four DGCMGs with the inner and outer gimbal angles α_i and β_i of the ith CMG, as defined in Fig. 11. The total CMG momentum vector $\boldsymbol{H} = (H_x, H_y, H_z)$ is expressed in the (x, y, z) axes as

$$\boldsymbol{H} = \begin{bmatrix} \sum \sin\alpha_i \\ \sum \cos\alpha_i \cos\beta_i \\ \sum \cos\alpha_i \sin\beta_i \end{bmatrix} \tag{28}$$

where a constant unit momentum is assumed for each CMG. The time derivative of $\boldsymbol{H}$ becomes

$$\dot{\boldsymbol{H}} = \begin{bmatrix} \sum \cos\alpha_i \dot{\alpha}_i \\ \sum(-\sin\alpha_i \cos\beta_i \dot{\alpha}_i - \cos\alpha_i \sin\beta_i \dot{\beta}_i) \\ \sum(-\sin\alpha_i \sin\beta_i \dot{\alpha}_i + \cos\alpha_i \cos\beta_i \dot{\beta}_i) \end{bmatrix} \tag{29}$$

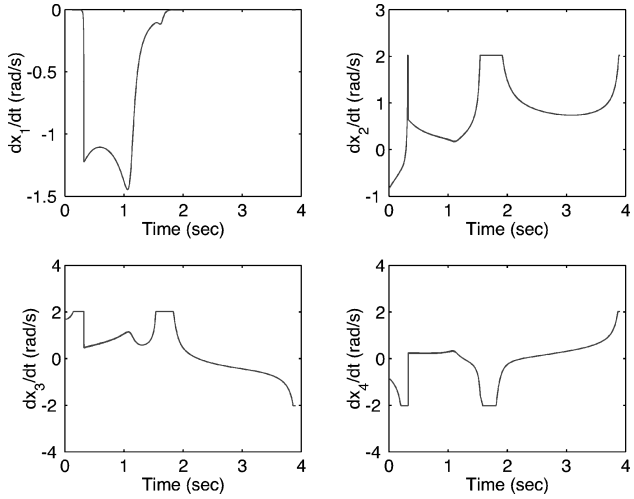

Fig. 10 Gimbal-rate time histories with a gimbal rate limit of ±2 rad/s.

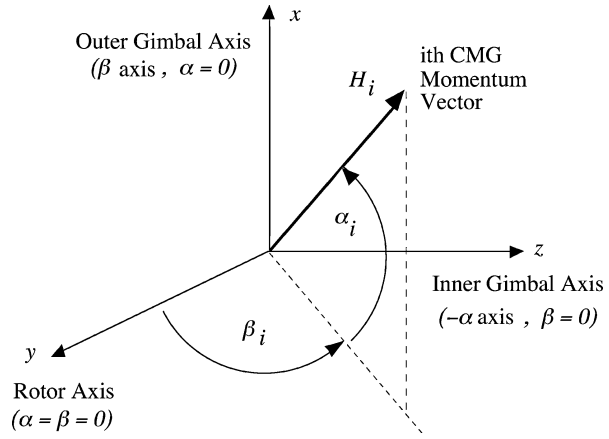

Fig. 11 Inner gimbal angle α_i and outer gimbal angle β_i of ith DGCMG.

Note that the x-axis torque component is not a function of the outer gimbal β_i motions. Consequently, in Kennel's CMG steering law[11] implemented on the International Space Station, the inner gimbal rate commands $\dot{\alpha}_i$ are determined first for the commanded x-axis torque then the outer gimbal rate commands $\dot{\beta}_i$ for the commanded y- and z-axis torques (also see Ref. 9).

Typical singularities of a system of four parallel DGCMGs are shown in Fig. 12. The 4H saturation singularity is an elliptic singularity that cannot be escaped by null motion. The 2H and 0H singularities, shown in Figs. 12b and 12c, respectively, are hyperbolic singularities that can be escaped by null motion. A nonsingular configuration but with a zero momentum is also shown in Fig. 12d.

The new steering logic of the form (13) can also be employed for a system of four parallel DGCMGs described by $\boldsymbol{A}\dot{\boldsymbol{x}} = \boldsymbol{\tau}$, where $\boldsymbol{x} = (\alpha_1, \alpha_2, \alpha_3, \alpha_4, \beta_1, \beta_2, \beta_3, \beta_4)$, $\boldsymbol{\tau} = (\tau_x, \tau_y, \tau_z)$, and $\boldsymbol{A}$ is a 3×8 Jacobian matrix, which can be easily constructed from Eq. (29).

The saturation singularity escape capability of the new steering logic is shown in Fig. 13. The simulation conditions for this case are initial gimbal angles $\alpha_i = \beta_i = 0$ for all i, commanded torque $(\tau_x, \tau_y, \tau_z) = (0, 1, 0)$, $\boldsymbol{W} = \text{diag}\{1, 1, 2, 2, 1, 1, 2, 2\}$, and $\boldsymbol{V} = \lambda \boldsymbol{E}$ with $\lambda = 0.01 \exp[-\det(\boldsymbol{A}\boldsymbol{A}^T)]$ and $\epsilon_i = 0.1 \cos t$. In Fig. 13, we have $\alpha_1 = \alpha_2 > 0$, $\alpha_3 = \alpha_4 < 0$, and $\beta_1 = \beta_2 > 0$, $\beta_3 = \beta_4 < 0$. For this case, the proposed steering logic escapes the saturation singularity but it passes through the 0H singularity, as can be seen in Fig. 13. However, for $\boldsymbol{W} = \boldsymbol{I}$ with any $\boldsymbol{V}$, this system remains singular at its singular momentum envelope, that is, the steering logic of Refs. 7 and 8 is unable to escape the saturation singularity of this system of four DGCMGs even when CMG momentum desaturation is requested.

Furthermore, when we choose $\boldsymbol{W} = \text{diag}\{1, 2, 3, 4, 1, 2, 3, 4\}$ and the same $\boldsymbol{V}$ as before, it can be seen in Fig. 14 that it escapes

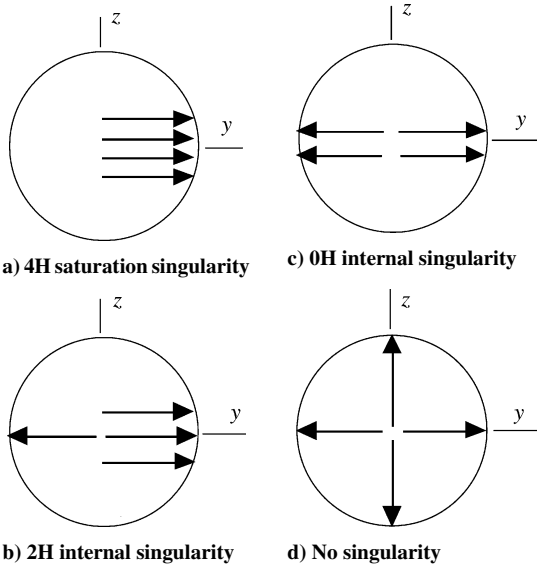

Fig. 12 Singularities of a system of four parallel DGCMGs.

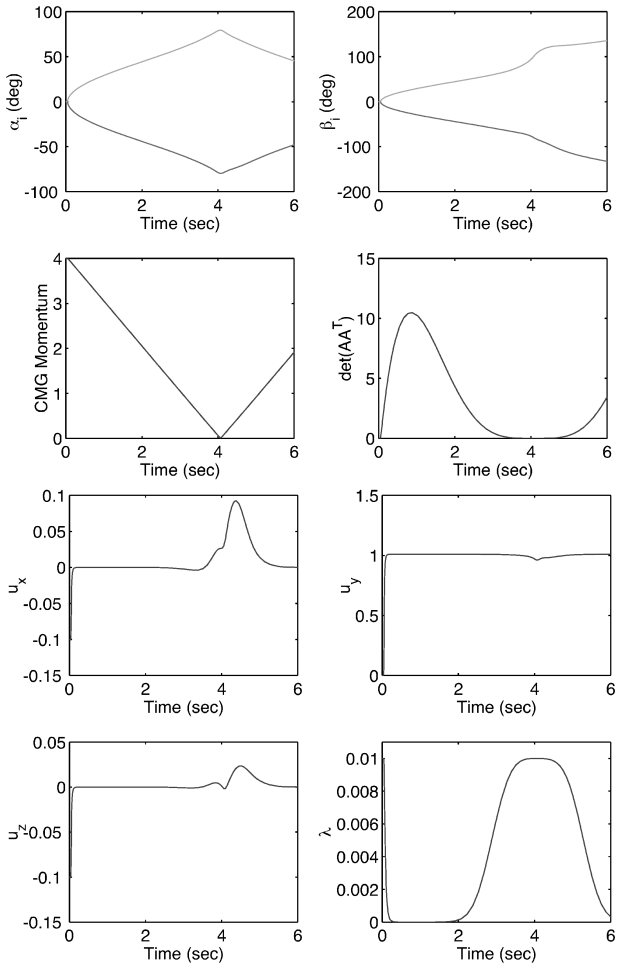

Fig. 13 Momentum desaturation simulation results for escaping 4H saturation singularity but passing through 0H singularity of four parallel DGCMGs with $W = \text{diag}\{1, 1, 2, 2, 1, 1, 2, 2\}$.

the saturation singularity and that the 0H singularity is completely avoided with no transient torque errors. The CMG momentum is completely desaturated at $t = 4$ s, but the desaturation torque is continuously commanded even after $t = 4$ s to further explore any problem of encountering an internal singularity.

This example of a system of four DGCMGs demonstrates that it is feasible to avoid singularity encounters completely (with no transient torque errors) with a proper selection of $\boldsymbol{W}$,

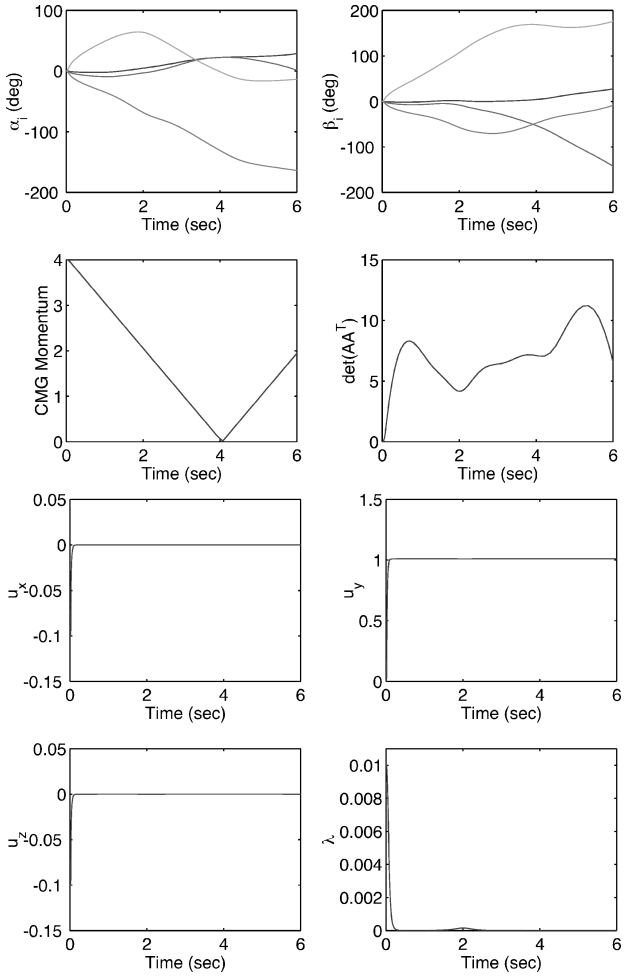

Fig. 14 Momentum desaturation simulation results for escaping saturation singularity and avoiding 0H singularity of four parallel DGCMGs with $W = \text{diag}\{1, 2, 3, 4, 1, 2, 3, 4\}$.

in conjunction with the deterministic dither signals generated in $\boldsymbol{V}$.

Simulation results also show that the new steering logic rapidly transits through the 2H singularity shown in Fig. 12b.

Mixed Single Gimbal CMG/DGCMG System

Four parallel mounted DGCMGs with a total weight of about 2400 lb and with a design life of 10 years are employed on the International Space Station (ISS). However, one of the ISS's four CMGs failed on 8 June 2002 after a little more than a year through its planned 10-year service life. Consequently, there is a possibility of augmenting the existing three DGCMGs of the ISS with an array of much smaller single gimbal CMGs (SGCMGs) manufactured by Honeywell. The proposed steering logic is directly applicable to such a mixed SGCMG/DGCMG system. Simulation results indicate that both $\boldsymbol{W}$ and $\boldsymbol{V}$ provide a simple yet effective way of combining DGCMGs with much smaller SGCMGs for a possible application to the ISS.

V. Conclusions

A new steering logic has been developed to overcome a deficiency of the previous singularity-robust steering logic of Wie et al.[7,8] The new steering logic uses an additional weighting matrix in conjunction with the deterministic dither signals in the singularity-robust steering logic. It can also be employed to avoid explicitly singularity encounters for which most other pseudoinverse-based steering logic either fail or must transit through. The practicality, effectiveness, and simplicity of the new singularity escape/avoidance logic, even in the presence of gimbal-rate limit, were demonstrated for

various CMG systems. The proposed steering logic can also be effectively employed for a mixed SGCMG/DGCMG system.

Acknowledgments

The author thanks the Reviewers and the Associate Editor, Hari Hablani, for their comments and suggestions for significantly improving the quality of this paper. Special thanks also go to Vaios Lappas and Philip Palmer for providing the author with an opportunity to further explore the control moment gyro steering control problem during his sabbatical leave at the Surrey Space Centre, University of Surrey, Guildford, England, United Kingdom.

References

[1]Damilano, P., "Pleiades High Resolution Satellite: a Solution for Military and Civilian Needs in Metric-Class Optical Observation," 15th Annual AIAA/USU Conf. on Small Satellites, Paper SSC01-I-5, Aug. 2001.

[2]Girouart, B., Sebbag, I., and Lachiver, J.-M., "Performances of the Pleiades-HR Agile Attitude Control System," *Proceedings of the 5th International ESA Conference on Spacecraft Guidance, Navigation and Control Systems*, European Space Research and Technology Center, Noordwijk, The Netherlands, 2002.

[3]Defendini, A., Faucheux, P., Guay, P., Morand, J., and Heimel, H., "A Compact CMG Products for Agile Satellites," *Proceedings of the 5th International ESA Conference on Spacecraft Guidance, Navigation and Control Systems*, European Space Research and Technology Center, Noordwijk, The Netherlands, 2002.

[4]Wie, B., Heiberg, C., and Bailey, D., "Rapid Multi-Target Acquisition and Pointing Control of Agile Spacecraft," *Journal of Guidance, Control, and Dynamics*, Vol. 25, No. 1, 2002, pp. 96–104.

[5]Lappas, V. J., Steyn, W. H., and Underwood, C. I., "Laboratory Experiments of a Control Moment Gyroscope Cluster for Agile Small Satellites," *Proceedings of the 5th International ESA Conference on Spacecraft Guidance, Navigation and Control Systems*, European Space Research and Technology Center, Noordwijk, The Netherlands, 2002.

[6]Wie, B., "Singularity Analysis and Visualization of Single-Gimbal Control Moment Gyro Systems," *Journal of Guidance, Control, and Dynamics*, Vol. 27, No. 2, 2004, pp. 271–282.

[7]Wie, B., Heiberg, C., and Bailey, D., "Singularity Robust Steering Logic for Redundant Single-Gimbal Control Moment Gyros," *Journal of Guidance, Control, and Dynamics*, Vol. 24, No. 5, 2001, pp. 865–872.

[8]Wie, B., Bailey, D., and Heiberg, C., "Robust Singularity Avoidance in Satellite Attitude Control," U.S. Patent 6,039,290, 21 March 2000.

[9]Wie, B., *Space Vehicle Dynamics and Control*, AIAA Education Series, AIAA, Reston, VA, 1998, pp. 435–445.

[10]Wie, B., "Singularity Escape/Avoidance Steering Logic for Control Moment Gyro Systems," U.S. Patent No. 6,917,862, 12 July 2005.

[11]Kennel, H. F., "Steering Law for Parallel Mounted Double-Gimballed Control Moment Gyros: Revision A," NASA TM-82390, Jan. 1981.